Catal Lett (2012) 142:1098–1106
DOI 10.1007/s10562-012-0865-6

Influence of Copper Loading on the Surface Species and Catalytic Properties in the Formation of Oxygenated By-products During FTS Over FeCuKLa/SiO_2 Catalysts

Wan-Yu Mao · Hong-Fang Ma · Hai-Tao Zhang · Qi-Wen Sun · Wei-Yong Ying · Ding-Ye Fang

Received: 18 April 2012 / Accepted: 23 June 2012 / Published online: 10 July 2012

Abstract The influence of copper loading on the surface species and catalytic properties of Fe–Cu–K–La/SiO_2 catalyst in the formation of oxygenated by-products during Fischer–Tropsch synthesis was investigated by temperature-programmed reduction (TPR), temperature-programmed desorption of CO and acetaldehyde (CO-, acetaldehyde-TPD), in situ diffuse reflectance FTIR and chemical trapping. The results showed that addition of copper improved the reducibility of catalysts, however, the adsorption features of catalysts changed significantly. Fe–Cu–K–La–SiO_2 with a composition of 1:0.28:0.05:0.05:0.17 (molar ratio, relative to iron) had highest selectivity for hydrocarbons and lowest selectivity for C_2^+ oxygenates. Results of FTIR and chemical trapping indicated that extra copper would suppress CO adsorption as well as oxidation of adsorbed molecules. The stability of intermediates weakened simultaneously. Moreover, the quantitative estimates of the concentration of the surface species by acetaldehyde-TPD allowed the illustration of copper effect on the catalytic properties.

Keywords Fischer–Tropsch · Oxygenated by-products · Surface species · Copper effect · Iron catalysts · DRIFT · Chemical trapping

W.-Y. Mao · H.-F. Ma · H.-T. Zhang · W.-Y. Ying (✉) · D.-Y. Fang
Engineering Research Center of Large Scale Reactor Engineering and Technology, Ministry of Education, State Key Laboratory of Chemical Engineering, East China University of Science and Technology, Shanghai 200237, China
e-mail: wying@ecust.edu.cn

Q.-W. Sun
State Key Laboratory of Coal Liquefaction and Coal Chemical Technology, Shanghai 201203, China

1 Introduction

The Fischer–Tropsch synthesis (FTS), first developed in Germany in 1923 [1] and now successfully applied at large scale by SASOL and Shell [2], is considered to be an important technology for the synthesis of liquid fuels and chemicals from syngas. A number of papers have concerned high performance catalysts for FTS including iron and cobalt [3–6]. In particular, iron-based catalysts have attracted much attention due to their high olefin selectivity, excellent stability and low cost [7–9]. A characteristic of iron-based catalyst is that their behavior strongly depends on composition, preparation and reaction conditions, which determine the iron phase composition and surface structures of the working catalyst [10].

Copper being a common promoter in applications to iron-based catalysts has been proposed to facilitate reduction of iron oxides during activation and minimize the sintering of iron by lowering the reduction temperature [11–13]. Although the role of copper in facilitating reducibility of catalysts has been widely accepted, a large number of C_2^+ oxygenates are formed which have often been considered as unimportant by-products of the synthesis. Influence of copper concentration on surface species and reactivity in the formation of oxygenated by-products has not been well addressed. O'Brien et al. [14] and Wachs et al. [15] pointed out that copper had no effect on product selectivity. However, noticeable alcohol selectivity was reported on FeCuKB catalyst [16] and $FeCuMnZrO_2$ catalyst [17]. Theoretical predictions supported by experimental results had shown that the selectivity to C_2^+ oxygenates was mainly determined by the extent of CH_3 trapped by an acyl [18, 19]. A determination on the effect of copper concentration is necessary to define the relationship between surface species and reactivity in the formation of oxygenated by-products during FTS.

The purpose of this paper is to study the influence of copper loading on the surface species and catalytic properties in the formation of oxygenated by-products during FTS over Fe-Cu-K-La/SiO_2. For this purpose, the characterization of the catalysts was carried out by temperature-programmed reduction (TPR), temperature-programmed desorption of CO and acetaldehyde (CO-, acetaldehyde-TPD), in situ diffuse reflectance FTIR and chemical trapping. The correlation between the surface species and the activity of these catalysts was also discussed.

2 Experimental

2.1 Catalyst Preparation

Catalysts were prepared by conventional co-precipitation method. Typically, a mixture of the related metallic nitrates and SiO_2 sol was co-precipitated with a NH_4OH solution at 343 ± 1 K and a constant pH of 7.5 ± 0.2. After aging for 12 h, the precipitate was washed thoroughly with deionized water, dried at 383 K for 24 h and then calcined at 753 K in air for 5 h. The composition of the catalysts were as follows: Fe:Cu:K:La:SiO_2 = 1:x:0.05:0.05:0.17 (molar ratio, x = 0.08, 0.18, 0.28, 0.31, 0.48). The compositions of all samples were determined by ICP-AES emission spectrometry.

2.2 Catalyst Characterization

TPR was conducted to study the reducibility of catalysts. They were performed with Autochem II 2920 model multifunctional adsorption instrument (Micromeritics Company, USA). Typically, the samples (0.1 g) were flushed at 773 K in a helium flow of 50 ml min^{-1} for 30 min, and then cooled to 323 K. After stabilization, the temperature was raised with a slope of 10 K min^{-1} up to 1173 K under a 30 ml min^{-1} 10 % H_2 in Ar mixture. The hydrogen consumption was calculated by comparison of the area of their TPR profiles and the profile of the standard sample of CuO.

Temperature-programmed desorption of CO or acetaldehyde was performed in the same equipment as used in the TPR tests. The catalysts were reduced in situ at 493 K during 6 h under a 1 l h^{-1} g_{cat}^{-1} hydrogen flow. 1.01 %CH_3CHO/He or CO was adsorbed at 308 and 393 K respectively. The catalytic surface was then flushed by a He flow for 2 h. Each experiment was performed in a He flow (2 l h^{-1} g_{cat}^{-1}) with an on-line GC–MS (model 7890A-5975C; Agilent) as a detector to monitor the desorbed species. CO, CO_2, CH_4 were analyzed with a HP-PLOT-Q column (30 m × 0.32 mm × 20 μm) and a thermal conductivity detector (TCD). CH_3CHO, CH_3OH, CH_3COCH_3 were measured with a HP-INNOWax column (30 m × 0.32 mm × 25 μm) and an FID. The temperature increasing rate was 3 K min^{-1}.

DRIFT analysis was carried out with a spectrometer (Nicolet 6700, Thermo, USA), fitted with an in situ cell which was connected to a feed system with a set of stainless steel gas lines, allowing in situ measurements. The infrared cell was equipped with temperature controlled parts and ZnSe window. The catalyst was reduced in situ for 6 h under atmospheric pressure by a stream of hydrogen at 493 K (30 ml min^{-1}, 1 K min^{-1}). Then the reactor was flushed by pure nitrogen. CO was introduced at room temperature under a pressure of 10^4 Pa. Acetaldehyde and methanol were also introduced at room temperature on reduced samples. The in situ reaction studies were performed under a hydrogen and carbon monoxide gas flow with a 2/3 molar ratio. After activation, the CO + H_2 gases were introduced and the spectra were recorded with the increasing temperature and pressure. After the system reached the steady state of 553 K and 3.5 MPa, it was flushed by N_2. Then the gas flow was switched to pure H_2.

The device used for chemical trapping experiments was the same to that used in DRIFT analysis. The species were trapped at 553 K by an excess of CH_3I.

All spectra were recorded with a resolution of 4 cm^{-1} and accumulation of 64 scans. Those reported in the figures were subtracted from the reference one.

2.3 Reactivity Measurements

The catalytic performance tests were conducted in a fixed-bed, stainless flow micro-reactor (6 mm I.D.) with a catalyst weight of 0.5 g. For all experiments, the samples were reduced in a hydrogen flow (1 l h^{-1} g_{cat}^{-1}) at 493 K at ambient pressure for 6 h before syngas exposure. Then the temperature was decreased to 473 K and the pressure was gradually increased to 4.0 MPa in H_2 atmosphere. The steady-state reaction conditions were set as 543 K, 4.0 MPa, H_2/CO = 2/3 and 4 l h^{-1} g_{cat}^{-1}. The carbon balance was 100 ± 5 %.

3 Results and Discussion

3.1 Temperature Programmed Reduction of H_2 (H_2-TPR)

The TPR profiles of Fe–Cu–K–La/SiO_2 catalysts with different copper loadings were shown in Fig. 1. The reduction peak maximums for the systems were situated at 473 K. High-temperature TPR profile showed a broad peak.

The amount of H_2 consumed during different reduction stages, obtained from integrating the area of the

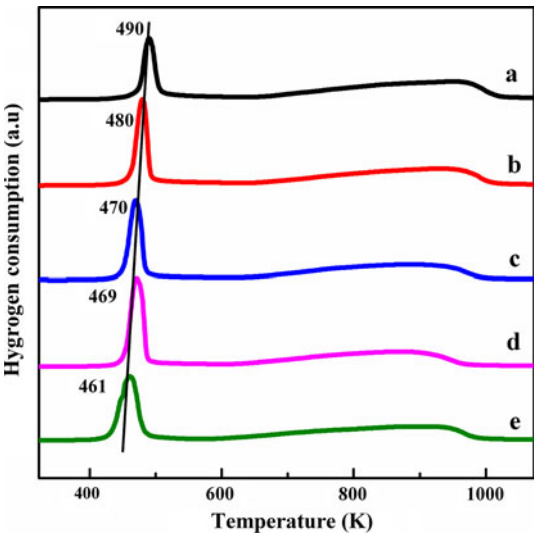

Fig. 1 Temperature-programmed reduction (H_2-TPR) spectra of Fe–Cu–K–La/SiO_2 catalyst with different copper loadings: (*a*) 0.08; (*b*) 0.18; (*c*) 0.28; (*d*) 0.31; (*e*) 0.48

Table 1 Quantitative results of H_2 consumption for catalysts in H_2-TPR

Catalysts	Peak (K)	H_2 consumption	
		mol H_2/mol M[a]	mol H_2/mol Fe
FeKLa–0.08Cu/SiO_2	490	0.22	
	950		1.03
FeKLa–0.18Cu/SiO_2	480	0.30	
	931		1.17
FeKLa–0.28Cu/SiO_2	470	0.32	
	888		1.25
FeKLa–0.31Cu/SiO_2	469	0.35	
	870		1.25
FeKLa–0.48Cu/SiO_2	461	0.38	
	914		1.31

The H_2 consumption was measured from the area under the corresponding peak

[a] M = Fe + Cu + La

corresponding reduction peak, was summarized in Table 1. For the five catalysts, the amounts of H_2 consumption for reduction peaks at lower temperature range (below 800 K) were close to the theoretical value for the combined reduction of CuO to Cu, La_2O_3 to LaO and Fe_2O_3 to Fe_3O_4 (0.24, 0.31, 0.35, 0.37, 0.44 mol H_2/mol M with the increased loadings of copper). The wide and asymmetric peaks at higher temperature (above 800 K) corresponded to the reduction of Fe_3O_4 to FeO and then to metallic iron [20], and the H_2 consumptions were consistent with theoretical values (1.33 mol H_2/mol Fe). FeO (Wüstite) was a metastable phase of iron oxides below 843 K [21] and had been reported on various supported catalysts [22, 23]. Munteanu et al. [24] calculated kinetic parameters of reduction process of Fe_2O_3 and found that the activation energy and rate constants for $Fe_3O_4 \rightarrow FeO$ and $FeO \rightarrow Fe$ were similar, which indicated that Fe_3O_4 reduced to Fe directly. Thus the TPR profile showed a wide peak for the reduction of Fe_3O_4.

The reduction temperature of CuO was between 423 and 473 K, much lower than that of Fe_2O_3 (about 573 K). CuO reduced to metallic state first and formed sites of nucleation which in turn led to reactive hydrogen species capable of reducing iron oxides at relatively low temperatures. Such a reduction process of iron oxide was well known as a nucleation model [25, 26]. Wachs et al. [27] had studied the effects of copper on the hydrogen reduction of α-Fe_2O_3 and found that copper was well dispersed on the catalyst surface and was concluded to provide more sites of nucleation for reduction to occur. It could be seen from Fig. 1 that increase of copper loading made the onset of the reaction sequences shifted from 490 to 461 K, indicating an easier reduction process for Fe_2O_3. Further, the H_2 consumption of Fe_2O_3 increased with the increased copper loading which confirmed the view that the reduction of the catalyst was strongly enhanced by copper.

3.2 Reaction Performance

Results of FTS over Fe–Cu–K–La/SiO_2 catalysts with different loadings of copper were shown in Fig. 2. The selectivity towards hydrocarbons first increased with the copper loading, then reached a maximum at copper amount of 0.28 (molar ratio, relative to iron, the same hereinafter), then decreased rapidly. Moreover, the higher alcohols (C_2^+ OH) and hydrocarbons (C_2^+ HC) yields decreased with the amount of copper. Such a simultaneous change had also been reported on cobalt-based catalysts by Takeuchi et al. [28], and on copper-based catalysts by Chu et al. [29]. A common intermediate for these two species was proposed [30]. Thus it was reasonable to conclude that copper on the surface can influence the chain growth both to hydrocarbons and alcohols.

3.3 CO Adsorption and Desorption

3.3.1 Infrared Spectra of CO Adsorption

The FTIR spectra obtained after CO adsorption on iron-based catalysts were shown in Fig. 3. The gas phase spectrum had been subtracted. One sharp band at 2,094 cm^{-1} was observed, corresponding to CO linearly adsorbed on surface [31]. The band showed a red shift with the rise of copper loading. This suggested that a kind of homogeneous site formed on the surface due to the addition of copper [32]. Band at 2,013 cm^{-1} could be assigned to

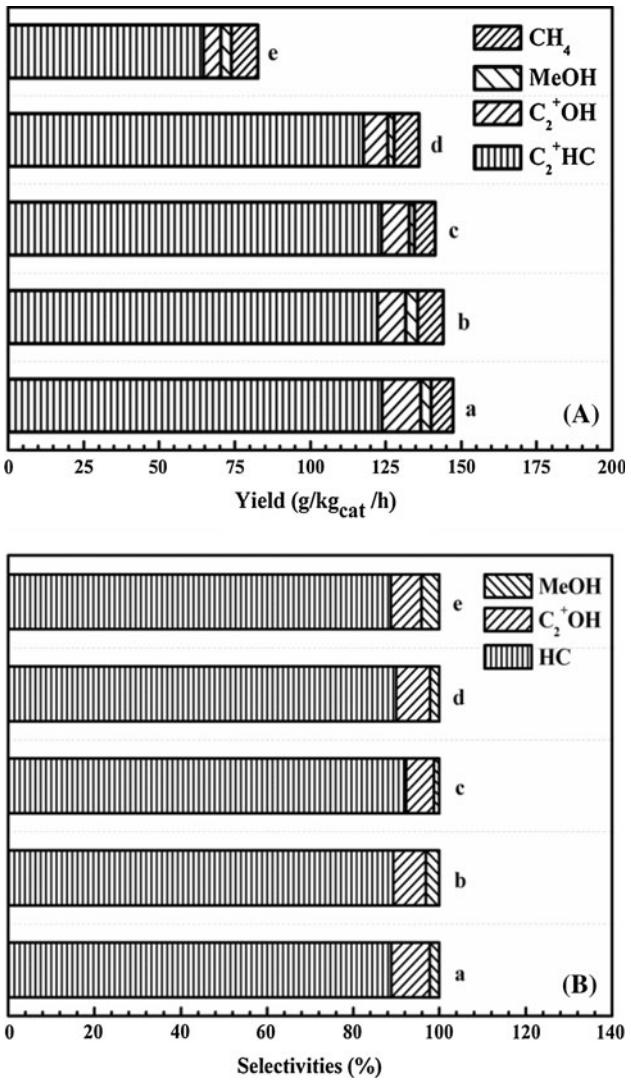

Fig. 2 Yield (**A**) and selectivity (**B**) of Fe–Cu–K–La/SiO_2 catalyst with different copper loadings: (*a*) 0.08; (*b*) 0.18; (*c*) 0.28; (*d*) 0.31; (*e*) 0.48. Reaction conditions: $H_2/CO = 2/3$, 4 l h^{-1} g_{cat}^{-1}, $P =$ 4.0 MPa, T = 543 K

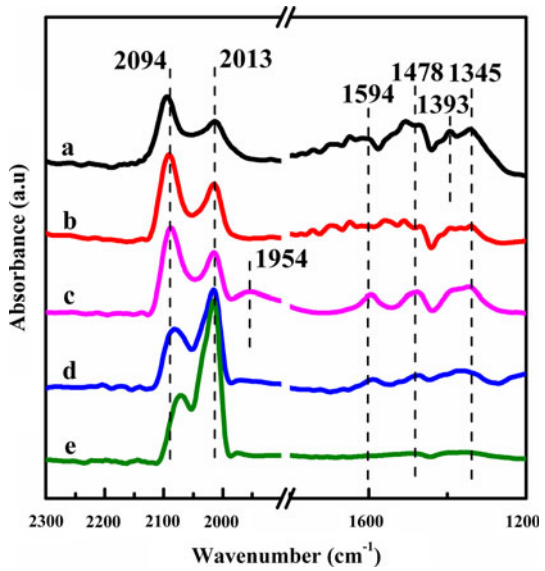

Fig. 3 FTIR spectra of CO adsorption at 298 K on Fe–Cu–K–La/SiO_2 catalyst with different copper loadings: (*a*) 0.08; (*b*) 0.18; (*c*) 0.28; (*d*) 0.31; (*e*) 0.48

the symmetric stretching mode of gem-dicarbonyl species. The characteristic band of asymmetric stretching mode of gem-dicarbonyl was situated at around 2,100 cm^{-1}. Its broadness was partly overlapped with that due to CO linearly adsorbed species. The bands corresponding to CO bridge-bonded species on iron sites were situated at the region of 1,900–1,975 cm^{-1} [33]. The band of bridge bonded species was apparently observed on Fe–Cu–K–La–SiO_2 with a composition of 1:0.28:0.05:0.05:0.17. This indicated that the surface adsorption sites of iron were enhanced. Further, it was generally considered that CO bridge bonded species were easily dissociated to oxygen and carbon. They were more active than the linear ones and favored to chain growth [34, 35]. Therefore, the high reactivity of Fe–K–La–0.28Cu/SiO_2 seemed to be associated with the enhancement of adsorption sites and formation of bridged-form CO. This result was in agreement with that of reactivity measurements.

The IR bands between 1,000 and 1,700 cm^{-1} had been assigned to carbonaceous species on surface which then underwent hydrogenation to produce bidentate carbonate (b-CO_3^{2-}) or bicarbonate (b-$HOCOO_s^-$) or formate species (b-$HCOO_s^-$), then methoxy species (CH_3O_s) [36, 37]. For CO adsorption on Fe-Cu-K-La/SiO_2 catalysts with low copper loading (0.08, 0.18 and 0.28), features attributed to b-$HOCOO_s^-$ (1,594 and 1,345 cm^{-1}) and b-$HCOO_s^-$ (1,478 and 1,393 cm^{-1}) were found. No characteristic bands were observed at higher copper loading (0.31, 0.48). Based on the results above, CO adsorption properties of the catalyst were influenced consumingly by addition of copper.

3.3.2 Temperature-Programmed Desorption of CO

TPD profiles of CO on Fe–Cu–K–La/SiO_2 with different copper loadings were shown in Fig. 4. Two peaks appeared at 418 and 575 K. Xu et al. [32] also observed two peaks during CO-TPD, which was consistent with those observed in this test, except that the shape of the profiles and the location of the peaks were not entirely identical. This seemed to be related to the different composition of the catalysts and TPD conditions. The two peaks shifted to higher temperature and the area of CO-TPD at higher temperature increased when the addition of copper increased within the range of 0.08–0.31. However, when the amount of copper exceeded 0.48, the CO desorption quantity would decrease. These implied that addition of

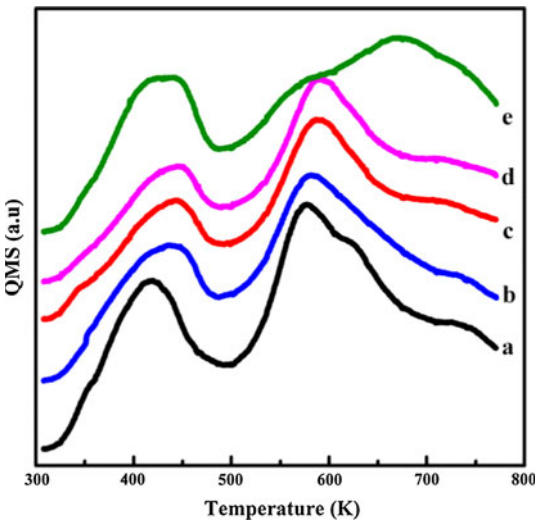

Fig. 4 TPD spectra after CO adsorption on Fe–Cu–K–La/SiO_2 catalyst with different copper loadings: (*a*) 0.08; (*b*) 0.18; (*c*) 0.28; (*d*) 0.31; (*e*) 0.48

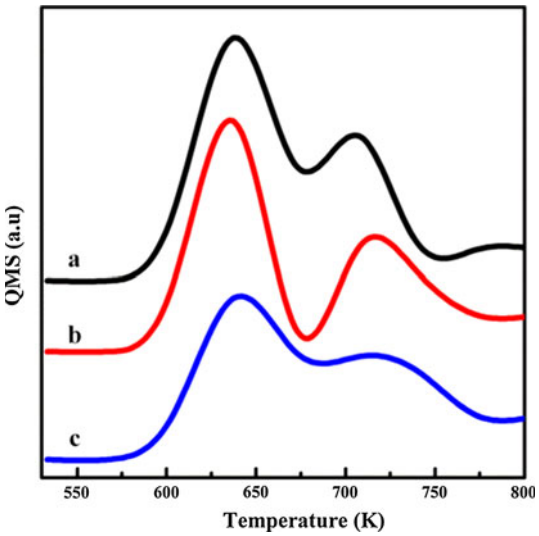

Fig. 5 Desorption spectra of CH_4 on Fe–Cu–K–La/SiO_2 catalyst with different copper loadings during TPD: (*a*) 0.08; (*b*) 0.31; (*c*) 0.48

0.08–0.31 copper to Fe–K–La/SiO_2 resulted in increase of the quantity of strongly adsorbed CO species, while extra copper would suppress CO adsorption on the iron surface. This was the reason that catalyst with high copper loading had low reactivity for CO hydrogenation.

For all the five catalysts, CO_2 was released in a large amount throughout the whole process and the profile appeared several desorption peaks. Desorption spectra of methane over Fe–Cu–K–La/SiO_2 with different copper loadings during TPD were shown in Fig. 5. A simultaneous desorption of methane occurred at around 673 K and the rate of methane formation dropped off sharply after maximum which may due to the depletion of adsorbed CO from the surface [38]. It was obvious that the formation of methane was caused by hydrogenation of the strongly adsorbed CO on surface. As shown in Fig. 5, the quantity of desorbed methane formed at higher temperature during TPD increased when the copper loading increased from 0.08 to 0.31. However, introduction of 0.48 copper to Fe–K–La/SiO_2 made the quantity decreased.

3.4 Methanol and Acetaldehyde Adsorption

FTIR spectra of adsorbed methanol on Fe–Cu–K–La/SiO_2 catalyst with different copper loadings were shown in Fig. 6. Bands appeared at 3006, 2948, 2843 and 1454 cm^{-1}. They could be attributed to methoxy species (ν_aCH_3 3,006 and 2,948 cm^{-1}, ν_sCH_3 2,943 cm^{-1}, δCH_3 1,454 cm^{-1}) compared with the results on the literature [39–41]. The features at 1601, 1321 and 762 cm^{-1} could be ascribed to ν_aO–C–O, ν_sO–C–O and δO–C–O vibration of formates respectively [42, 43]. The maximum amounts of formates were observed on Fe–K–La–0.28Cu/SiO_2 catalyst. However, the formation of formates would be suppressed when the amount of copper exceeded 0.48. It was known that formates were formed by oxidation of methoxy species. Such a result clearly indicated that extra copper would suppress the reactivity of oxidizing on adsorbed molecules. Further, features at 2,981 and 1,400 cm^{-1} decreased with the increased addition of copper. These bands were in good agreement with bands observed by Zamboni et al. [44]. These authors assigned these frequencies to linear or cyclic polymeric compounds. This indicated that the stability of such an intermediate weakened which may due to some extra copper covered the

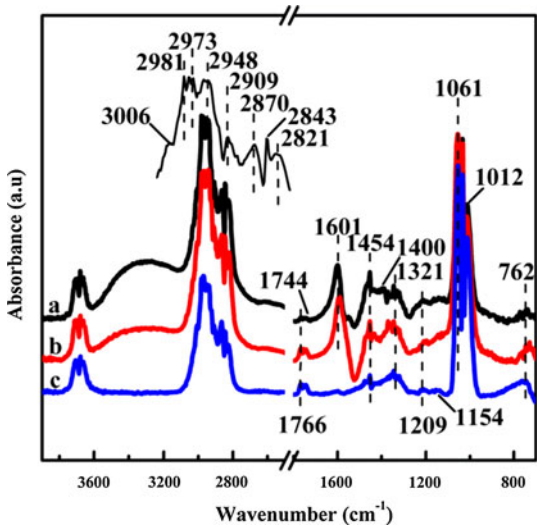

Fig. 6 FTIR spectra of CH_3OH adsorption on Fe–Cu–K–La/SiO_2 catalyst with different copper loadings: (*a*) 0.08; (*b*) 0.31; (*c*) 0.48

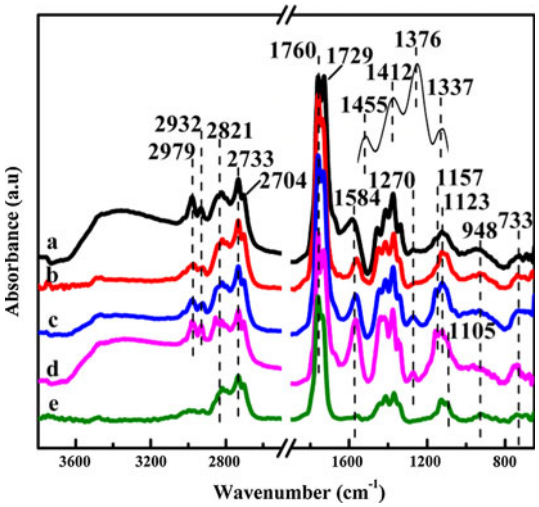

Fig. 7 FTIR spectra of acetaldehyde adsorption on Fe–Cu–K–La/SiO_2 catalyst with different copper loadings: (*a*) 0.08; (*b*) 0.18; (*c*) 0.28; (*d*) 0.31; (*e*) 0.48

surface of iron particles. On the contrary, band at 1,766 cm^{-1} and a shoulder at 1,744 cm^{-1} increased pronouncedly with the addition of copper. These two bands could be attributed to a C and O coordinated carbon monoxide. Bands at 2948 (ν_aCH_3), 2870 (Fermi resonance $2\delta CH_3$ and ν_sCH_3), 2821 (ν_sCH_3) and 1061 cm^{-1} (νC–O) were probably that of a bidentate methoxy species on surface [45].

Acetaldehyde was adsorbed on copper promoted Fe–K–La/SiO_2 catalyst at room temperature (Fig. 7). The adsorption gave rise to bands at 2979, 1455, 1159, 1123 (as a shoulder) and 948 cm^{-1}. These bands corresponded well to those observed during adsorption of formaldehyde on Ru(001) by Anton et al. [46] and had been attributed to an adsorbed CH_3CHO in η^2(C,O)CH_3CHO configuration (ν_aCH_3 2979 cm^{-1}, δCH_3 1455 cm^{-1}, ωCH_3 1123 cm^{-1}, νC–O 948 cm^{-1}). Bands due to physically and chemically adsorbed acetaldehyde were also observed and were situated at 1,729 and 1,584 cm^{-1} respectively. Their intensity developed simultaneously when the amount of copper increased from 0.08 to 0.28 and decreased dramatically when the copper loading reached 0.48. Similar trends could be found in the formation of formates (ν_sO–C–O 1376, 1337 cm^{-1}, δO–C–O 733 cm^{-1}) [42, 43]. Such a result corresponded well to those observed in the methanol adsorption. This confirmed the inference that extra copper would suppress oxidizing of adsorbed molecules. When the copper loading exceeded 0.31, a new band appeared at 1,105 cm^{-1}. This band together with the characteristic bands at 2932, 2821 and 1412 cm^{-1} could be assigned to bidentate methoxy species (ν_aCH_3 2932 cm^{-1}, ν_sCH_3 2821 cm^{-1}, δCH_3 1412 cm^{-1}, νC–O 1105 cm^{-1}).

3.5 Chemical Trapping

It is known that an acyl intermediate has often been proposed to be the key to the C_2-oxygenates formation [47–50] and can be trapped by CH_3I [51]. Thus we conducted chemical trapping studies: $CH_3I + H_2 + CO$ (Fig. 8).

Upon addition of syngas on Fe–Cu–K–La/SiO_2, the characteristic bands of adsorbed CO were observed at 2178 (gas-phase), 2114 (linear), 1918 and 1884 cm^{-1} (bridged). Addition of CH_3I resulted in peaks reduction at 2900, 2874, 1678, 1418 and 1104 cm^{-1} which corresponded to an acetyl [52] (νCH_3, νC=O, δ_sCH_3, δ_aC–C). Such a result indicated chemical trapping reactions (surface trapping of an acetyl species by a surface CH_3 entity) on the surface. This had been confirmed by the fact that νC=O vibration of an acetone which located at 1,615 cm^{-1} developed simultaneously, in agreement with the following scheme:

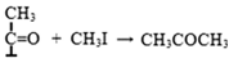

R1

Features corresponding to an acetate species were also observed (ν_aCH_3: 3014 and 2983 cm^{-1}, ν_sCH_3: 2937 cm^{-1}, ν_aO–C–O: 1518 cm^{-1}, ν_sO-C–O: 1450 cm^{-1}, δCH_3: 1338 cm^{-1}, ρCH_3: 1058 cm^{-1}, δ_aO–C–O: 942 cm^{-1}). We could find similar trends for acetate formation with that in methanol and acetaldehyde adsorption on Fe–Cu–K–La/SiO_2 catalyst with different copper

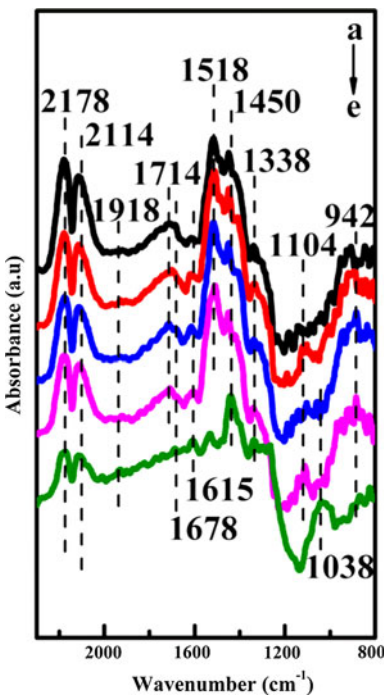

Fig. 8 FTIR spectra of $CH_3I + CO + H_2$ adsorbed on Fe–Cu–K–La/SiO_2 catalyst with different copper loadings: (*a*) 0.08; (*b*) 0.18; (*c*) 0.28; (*d*) 0.31; (*e*) 0.48: 553 K, t = 72 s

loadings. Further, the characteristic band for acetone showed a simultaneous development when addition of copper increased in range of 0.08–0.31. However, when copper was much more, its intensity would decrease.

Kiennemann et al. [18] had been proposed that surface CH_3 trapped by an acyl caused the low-temperature acetone (below 573 K) formation in acetaldehyde-TPD and the amount of such an acetone correlated with the formation of acetyl. To elucidate the role of those acetone, temperature-programmed desorption of acetaldehyde was conducted. The TPD spectra after chemisorption of acetaldehyde on FeKLa–0.48Cu/SiO_2 were shown in Fig. 9. TCD signals represented the cumulative signals of carbon monoxide, carbon dioxide, methane, water et al. analyzed with a built-in thermal conductivity detector. Such TPD data were corresponded well to results given by the authors who illustrated that three areas of desorption products could be observed including acetaldehyde and/or ethanol (353–393 K), acetone (about 473 K) and CO_2, CO, methane, acetone (573–673 K) [26]. It could be observed that on the copper modified iron catalysts, the ratio of the low-temperature acetone peak area to the total desorption peaks area had some relationships with the higher alcohols orientation and Table 2 gave the comparison between the two. However, the previous relationship established between the quantity of acetone and copper loading in the chemical trapping experiment was not found. This could be explained from the fact that chemical trapping taken at 553 K made some of the acetate desorbed and acetone observed in the FTIR consisted of two parts, one being formed by surface trapping of an acetyl, the other being formed from acetate decomposition. This result together with the reactivity measurements indicated that copper loading had a more complicated effect on the reactivity of the catalysts. On basis of acetaldehyde-TPD one could note that when the addition of copper was in range of 0.08–0.28, the selectivity and yield for C_2^+OH decreased simultaneously. This may due to the decreased quantity of low-temperature acetone. However, a slight increase in the selectivity and a continuous drop in the yield for C_2^+OH were observed when much more copper was added. This indicated that extra copper would suppress the activity of the catalysts more fiercely in spite of the slightly enhanced low-temperature acetone formation.

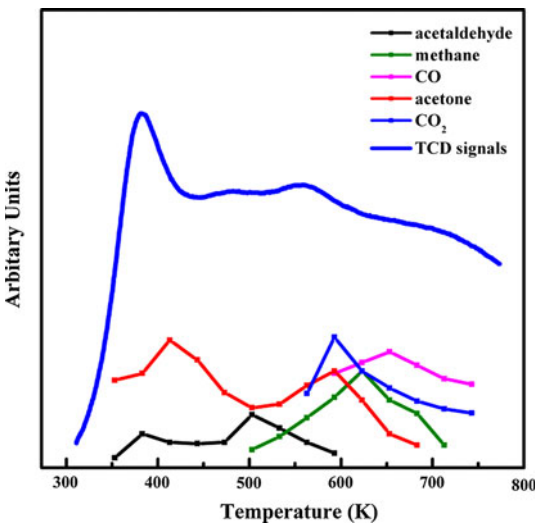

Fig. 9 TPD spectra after chemisorption of acetaldehyde on FeKLa–0.48Cu/SiO_2

Table 2 TPD after acetaldehyde adsorption: the higher alcohols orientation

Catalysts	$(CH_3)_2CO$[a]/total desorption peaks	C_2^+OH Selectivity (%)
FeKLa–0.08Cu/SiO_2	10.80	8.78
FeKLa–0.18Cu/SiO_2	8.56	7.53
FeKLa–0.28Cu/SiO_2	7.14	6.49
FeKLa–0.31Cu/SiO_2	8.88	7.91
FeKLa–0.48Cu/SiO_2	7.85	7.08

[a] Desorbed between 373 and 473 K

3.6 In Situ Reaction

The spectra obtained in the stationary conditions were presented in Fig. 10A. The characteristic bands of adsorbed CO and methoxy species were observed at 2127, 2012 cm^{-1} and 2931, 2866, 2827, 1031 cm^{-1} respectively. According to the results given in the previous chemical trapping experiments, bands at 3013, 2965, and 1465 cm^{-1} could be assigned to acetate species (ν_aCH_3, ν_sCH_3, ν_sO–C–O). By replacing $CO + H_2$ mixture with pure H_2 (1 atm) at 553 K, the band at 1,678–1,656 cm^{-1}, which partially overlapped with that due to bridge-bonded carbon monoxide, rapidly decreased. This band could be assigned to νC=O of the acetyl species formed in $CO + H_2$ reaction. Comparing the figures in Fig. 10A, B, one noted a sensitive decrease of the band at 2,931 cm^{-1} when the copper loading was in the region of 0.08–0.28. This result together with the disappearance of bands at 3,013 and 2,965 cm^{-1} indicated the acetate hydrogenation. Specially, when the addition of copper was 0.08, almost all the bands in the region of 3,000–2,800 cm^{-1} disappeared. However, extra copper caused no apparent changes toward hydrogen. This might point to an unfavorable mobility of products formed on the catalytic surface and could be associated with the reduced reactivity of Fe–Cu–K–La/SiO_2 catalyst with high copper loadings.

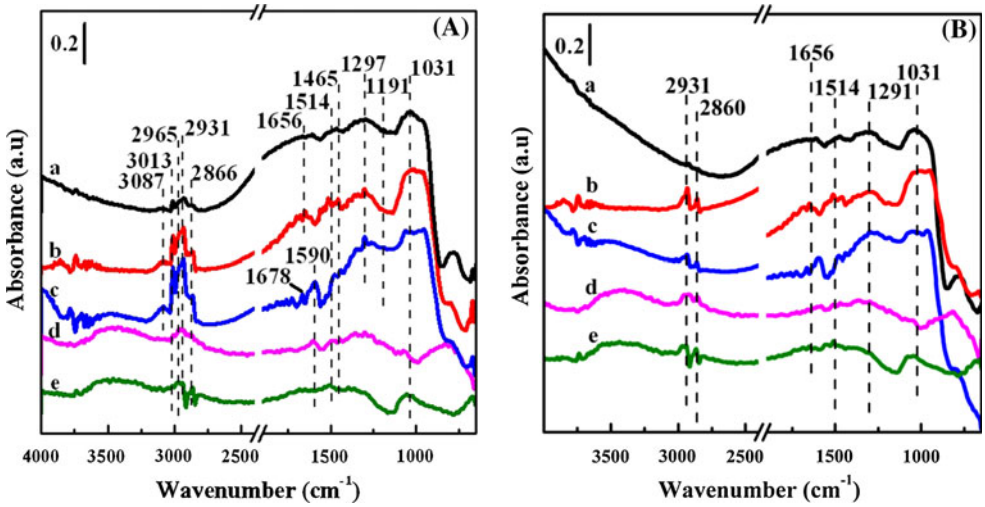

Fig. 10 FTIR spectra of adsorbed species formed from CO + H_2 interaction on Fe–Cu–K–La/SiO_2 catalyst with different copper loadings: (*a*) 0.08; (*b*) 0.18; (*c*) 0.28; (*d*) 0.31; (*e*) 0.48: (**A**) 553 K, 3.5 MPa; (**B**) spectra after switching to pure H_2

4 Conclusion

The effect of copper concentration on the surface species and catalytic properties of Fe–Cu–K–La/SiO_2 catalyst in the formation of oxygenated by-products during FTS was investigated by TPR, temperature-programmed desorption of CO and acetaldehyde (CO-, acetaldehyde-TPD), in situ diffuse reflectance FTIR and chemical trapping. It was found that adsorption features of catalysts changed significantly with the addition of copper. On the one hand, the presence of copper strongly enhanced the reduction of the catalysts which may resulted from the high probability of H_2 dissociation of copper and the interaction between iron and copper. However, CO adsorption on Fe–Cu–K–La/SiO_2 with extra copper loading was suppressed. CO bridge bonded species which were considered to be more active were visible only on Fe–Cu–K–La–SiO_2 with a composition of 1:0.28:0.05:0.05:0.17. On the other hand, detection of methanol and acetaldehyde adsorption in FTIR allowed us to imagine that the stability of oxygenated intermediates weakened and the reactivity of oxidizing of adsorbed molecules were suppressed when too much copper was added. Further, results of chemical trapping experiments as well as acetaldehyde-TPD were in good agreement with a scheme of surface trapping of an acetyl species by a surface CH_3 entity. These observed results together with the in situ reaction tests confirmed the inference that copper addition in an appropriate amount would increase the selectivity for hydrocarbons and decrease the selectivity for $C_2{}^+OH$. However, when much more copper was added, the activity of the catalysts would be suppressed fiercely. Thus, copper loading influenced the process of FTS. This effect would be reflected by the surface species formation and oxygenated by-products formation during the synthesis.

Acknowledgments The authors gratefully acknowledge the financial support of the Major State Basic Research Development Program of China (973 program, Grant No. 2010CB736203), the National High-Tech R&D program of China (863 program, Grant No. 2011AA05A204) and Shanghai Yankuang Energy R&D Co., Ltd.

References

1. Fischer F, Tropsch H (1923) Brennst Chem 4:276
2. Dry ME (2004) Appl Catal 276:1
3. Zhang CH, Yang Y, Teng BT, Li TZ, Zheng HY, Xiang HW, Li YW (2006) J Catal 237:405
4. Qin SD, Zhang CH, Xu J, Wu BS, Xiang HW, Li YW (2009) J Mol Catal 304:128
5. Borg Ø, Hammer N, Eri S, Lindvåg OA, Myrstad R, Blekkan EA, RØnning M, Rytter E, Holmen A (2009) Catal Today 142:70
6. Zhang H, Ma H, Zhang H, Ying W, Fang D (2012) Catal Lett 142:131
7. Barrault J, Renard C (1985) Appl Catal 14:133
8. Jiang M, Koizumi N, Yamada M (2000) J Phys Chem 104:7636
9. Yang Y, Xiang H, Xu Y, Bai L, Li Y (2004) Appl Catal 266:181
10. Butt JB (1990) Catal Lett 7:83
11. Grzybek T, Klinik J, Papp H, Baerns M (1990) Chem Eng Technol 13:156
12. Li S, Krishnamoorthy S, Li A, Meitzner GD, Iglesia E (2002) J Catal 206:202
13. Jin Y, Datye AK (2000) J Catal 196:8
14. O'Brien RJ, Xu L, Spicer RL, Bao S, Milburn DR, Davis BH (1997) Catal Today 36:325
15. Wachs IE, Duyer DJ, Iglesia E (1984) Appl Catal 12:201
16. Anderson RB, Seligman B, Schultz JF, Kelly R, Elliott MA (1952) Ind Eng Chem 44:391
17. Xu R, Yang C, Wei W, Li WH, Sun YH, Hu TD (2004) J Mol Catal 221:51
18. Kiennemann A, Barama A, Boujana S, Bettahar MM (1993) Appl Catal 99:175
19. Kiennemann A, Boujana S, Diagne C, Courty Ph, Chaumette P (1991) Natural gas conversion. Elsevier Inc., Amsterdam
20. Webb PA, Orr C (1997) Analytical methods in fine particle technology. Micromeritics Instrument Corporation, Cornell University, USA
21. Edstrom JO (1953) J Iron Steel Inst 175:289

22. Clausen BS, Topsøe H, Morup S (1989) Appl Catal 48:327
23. Kock AJHM, Fortuin HM, Geus JW (1985) J Catal 96:261
24. Munteanu G, Ilieva L, Andreeva D (1997) Thermochim Acta 291:171
25. Zhang CH, Yang Y, Tenga BT, Li TZ, Zheng HY, Xiang HW, Li YW (2006) J Catal 237:405
26. Lohitharn N, Goodwin JG Jr, Lotero E (2008) J Catal 255:104
27. Wachs IE, Dwyer DJ, Iglesia E (1984) Appl Catal 12:201
28. Takeuchi A, Katzer JR, Schuit GCA (1983) J Catal 82:351
29. Chu W, Kieffer R, Kiennemann A, Hindermann JP (1995) Appl Catal 121:95
30. Kiennemann A, Diagne C, Hindermann JP, Chaumette P, Courty Ph (1989) Appl Catal 53:197
31. Lavalley JC, Saussey J, Lamotte J (1990) J Phys Chem 94:5941
32. Xu R, Ma ZY, Yang C, Wei W, Li WH, Sun YH (2004) J Mol Catal 218:133
33. Sheppard N, Nguyen TT (1978) In: Clark RJH, Hester RE (eds) Advances in infrared and Roman spectroscopy, Vol 5, Chap 1. Wiley-Interscience, New York
34. Tsubaki N, Sun SL, Fujimoto K (2001) J Catal 199:236
35. Hindermann JP, Hutchings GJ, Kiennemann A (1993) Cat. Rev Sci Eng 3(5):1
36. Schild C, Wokaun A, Baiker A (1990) J Mol Catal 63:223
37. Weigel J, Koeppel RA, Baiker A, Wokaun A (1996) Langmuir 12:5319
38. Yin HM, Ding YJ, Luo HY, Zhu HJ, He DP, Xiong JM, Lin LW (2003) Appl Catal A 243:155
39. Davis JL, Barteau MA (1990) Surf Sci 235:235
40. Schild C, Wokaun A, Baiker A (1990) J Mol Catal 63:243
41. Greenler RG (1962) J Chem Phys 37:2094
42. Saussey J, Rais T, Lavalley JC (1985) Bull Soc Chim Fr :305
43. Sexton BA (1979) Surf Sci 88:319
44. Zamboni V, Zerbi G (1964) J Polym Sci 7:153
45. Binet C, Badri A, Lavalley JC (1994) J Chem Phys 98:6392
46. Anton AB, Parmeter JE, Weinberg WH (1986) J Am Chem Soc 108:1823
47. Underwood RP, Bell AT (1988) J Catal 111:325
48. Sachtler WMH, Ichikawa M (1986) J Phys Chem 90:4752
49. Anderson KG, Ekerdt JG (1985) J Catal 95:602
50. Hackenbruch J, Keim W, Roper M, Strutz H (1985) J Mol Catal 26:129
51. Chateau L, Hindermann JP, Kiennemann A, Tempesti E (1996) J Mol Catal 107:367
52. Hieber W, Braun G, Beck W (1960) Chem Ber 93:901